Polymer 49 (2008) 2903–2910

Contents lists available at ScienceDirect

Polymer

journal homepage: www.elsevier.com/locate/polymer

Synthesis and properties of paraffin capsules as phase change materials

Zhaoguo Jin, Yande Wang, Jiguang Liu*, Zhenzhong Yang*

State Key Laboratory of Polymer Physics and Chemistry, Institute of Chemistry, Chinese Academy of Sciences, Beijing 100190, China

ARTICLE INFO

Article history:
Received 9 January 2008
Received in revised form 2 April 2008
Accepted 13 April 2008
Available online 23 April 2008

Keywords:
Phase change materials
Capsules
In situ polymerization

ABSTRACT

Capsules containing paraffin as phase change core were in situ synthesized by the absorption and polymerization of urea–formaldehyde prepolymer onto the core in the presence of hydrolyzed styrene–maleic anhydride copolymer as emulsifier in aqueous phase. The particle size and shell content were controlled. A series of capsules in the form of powder have been synthesized with high thermal enthalpy capacity due to the high crystallization of the core paraffin. They were stable against coalescence after heating/cooling cycles. The capsules can find potential applications such as in energy conservation, functional heat fluid and heat protection materials.

1. Introduction

Phase change materials (PCMs) as a kind of crystalline materials, can store and release latent heat during their phase transition at a defined temperature range, which can be used in thermal energy conservation [1]. Paraffin wax is especially promising due to their characteristics such as nontoxic, chemically inert, low cost, and tunable phase change temperature and high storage energy capacity [1,2]. Paraffin wax has broad potential applications, such as in thermal regulated fabrics, coatings and foams [3–7], buildings [8,9], active or pumped coolants [10,11], and packed bed heat exchangers [12]. In order to prevent melt flowing during solid–liquid phase transition, encapsulation of PCMs with proper materials as shells is required. However, most studies are focused on the encapsulation of ambient temperature wax at low temperature [1]. For these PCMs with higher phase change temperature are scarcely reported. Moreover, these capsules have extensive potential application in solar energy storage [10], functional heat fluid [11], and heat protection materials [13,14] for high-performance management. In order to promote really utilization of PCM capsules, it is necessary to investigate in detail the fabrication and properties of PCM capsules.

Many methods have been searched for encapsulation of PCMs, such as in situ polymerization [15–18], interfacial polymerization [19] and complex coacervation [20]. Among these encapsulation methods, the in situ polymerization, which had also exhibited excellent function on preparing organic/inorganic composites, especially nanocomposite, is more favorable due to the resulted special structure and a series of capsules containing ambient temperature PCMs have been fabricated for thermal-regulated fibers [21–27] by in situ polymerization. However, how to make the polymerization in situ performed on the interface of PCMs and water is a key problem, which directly decides the shell structure of PCM microcapsules. Moreover, in order to avoid the shell fracturing by volume change during the phase transition [28], additional cyclohexane is usually used as an expansion agent to previously leave some free volume thus to improve thermal stability of the capsules. However, this expansion agent must be removed by evaporation, which involves additional steps and environmental pollution.

In this report, encapsulation of high melting temperature wax is reported by an in situ polymerization in the absence of any expansion agents. The fundamental nature of the polymerization and encapsulation is provided to well understand the shell-forming process. A detailed investigation on phase behavior of the encapsulated PCMs was performed to well understand the relation between the phase change stability of the as-prepared PCM capsules and shell materials. Thermal stability and enthalpy capacity are systematically characterized by differential scanning calorimeter (DSC) and polarized optical microscopy (POM).

2. Experimental

2.1. Materials

The paraffin with a phase change temperature range 50–52 °C, was purchased from Shanghai Huayong Paraffin Ltd., and chosen as a representative core material. Formaldehyde (37 wt% aqueous solution) and urea (Beijing Chemical Regent Co.) were used as precursors to form the shell. Styrene (distilled), maleic anhydride

* Corresponding authors. Fax: +86 10 62559373.
E-mail addresses: jiguangl@iccas.ac.cn (J. Liu), yangzz@iccas.ac.cn (Z. Yang).

0032-3861/$ – see front matter © 2008 Elsevier Ltd. All rights reserved.
doi:10.1016/j.polymer.2008.04.030

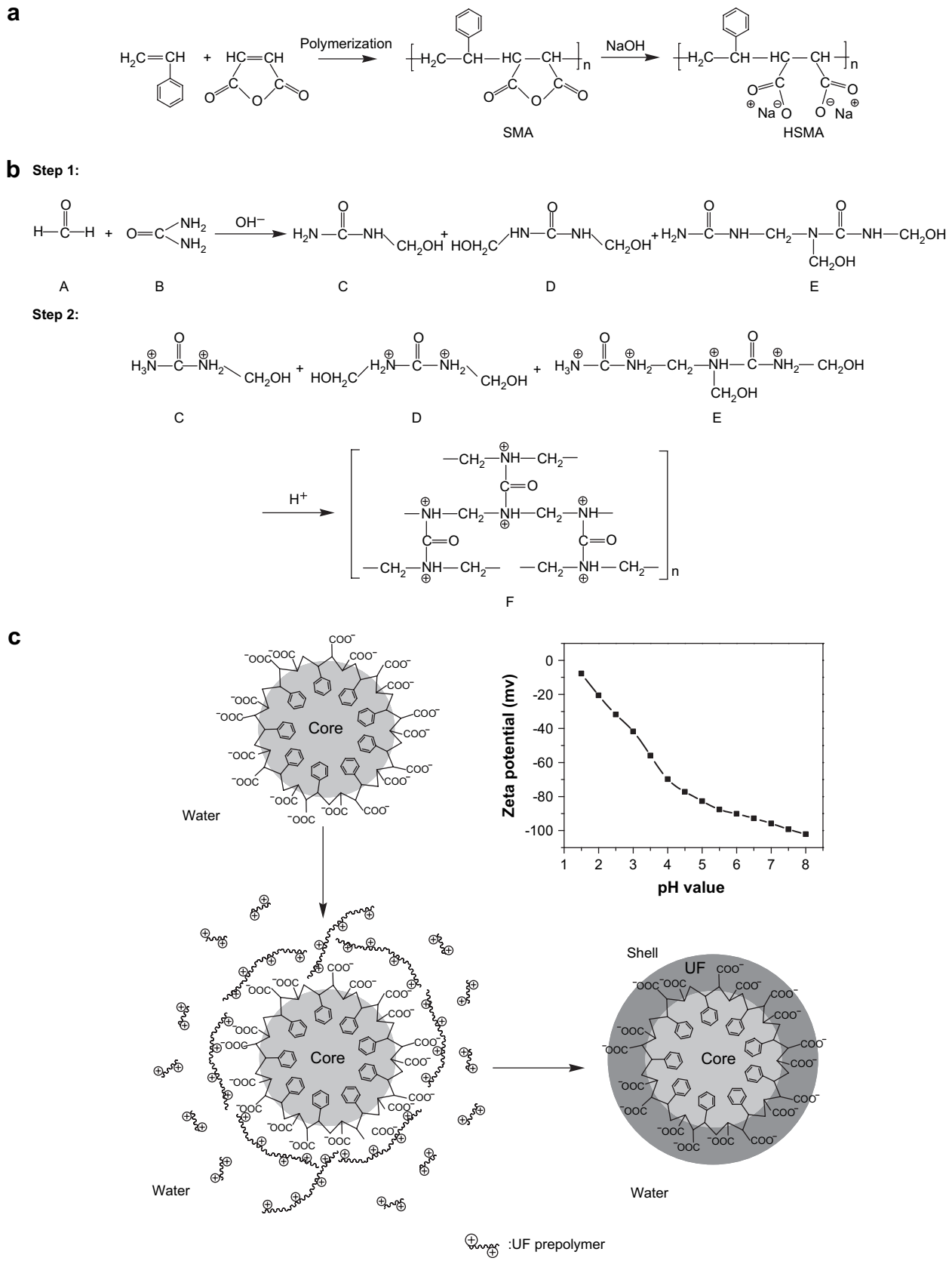

Fig. 1. Chemical structures of styrene–maleic anhydride (SMA) and its hydrolyzed form (HSMA) (a), chemical structures and reaction schemes of UF prepolymer and UF polymer (b), the zeta potential of the O/W emulsion with HSMA as the emulsifier at different pH values and illustrative emulsification and fabrication of PCM capsules (c).

and 2,2-azobis-(2-methylpropionitrile) (AIBN) (recrystallized from methanol prior to use) were purchased from Aldrich Chemical Co., used to synthesize styrene–maleic anhydride alternating copolymer (SMA) as the emulsifier.

2.2. Fabrication of capsules

2.2.1. Synthesis of the copolymer emulsifier

A copolymerization of styrene and maleic anhydride at 1:1 molar ratio was carried out by a precipitation polymerization method. In a 250 mL three-neck flask, 150 mL of toluene, 5.8 mL of styrene (0.051 mol), 5.0 g of maleic anhydride (0.051 mol) and 0.01 g of AIBN were added under stirring. After being purged with nitrogen for 30 min, the mixture was heated to 85 °C and refluxed for 2 h. The copolymer SMA (styrene–maleic anhydrite) was separated by filtration, and washed with toluene to remove residual reactants. The product was finally dried in an oven at 60 °C at a reduced pressure. The anionic emulsifier was obtained by the hydrolysis of the SMA copolymer. SMA powder (10.0 g) was dissolved in 90 g of 3 wt% sodium hydroxide solution under stirring at 80 °C for 3 h, deriving a transparent solution about 10 wt%, denoted as HSMA.

2.2.2. Synthesis of precursor

A precursor solution was prepared by mixing 24.0 g of urea and 48.9 g of 37 wt% formaldehyde in aqueous solution. The pH of the mixture was adjusted to 8.5 with triethanolamine and stirred at 70 °C for 1 h, and then the reaction mixture was cooled down to ambient temperature and diluted with 100.0 g of water. Sodium chloride (10 wt%) in respect to the precursor solution (denoted as UF) was added prior to use.

2.2.3. Synthesis of capsules

The encapsulation of the paraffin was carried out by an in situ polymerization. After a given amount of HSMA solution was dissolved in 75 mL of water, the solution was heated to 70 °C. Paraffin melt (25.0 g) was dispersed into the aqueous solution with a homogenizer at a stirring speed of 12 000 rpm for 10 min, forming an oil-in-water dispersion. Afterwards, a given amount of UF solution was dropped into the emulsion under stirring, and the reaction mixture was kept at pH 3.5–4.0 and 70 °C for 3 h to allow the in situ polycondensation. The resultant dispersion was cooled down to ambient temperature. After a sequential treatment including filtration, wash with water and drying at 60 °C in a vacuum oven, the PCM capsules were obtained.

2.3. Characterization

Gel Permeation Chromatography (GPC) was carried out to determine the M_n and M_w/M_n of SMA with linear polystyrene standards as the calibration and THF as eluent at a rate of 1.0 mL/min. ^{1}H NMR and ^{13}C NMR spectra were recorded on a Bruker DMX600 spectrometer with *d*-acetone as solvent at room temperature. The zeta potential on the latex surface of paraffin droplet emulsified by HSMA was measured on a Malvern ZetaSizer Nano ZS at pH 1.5–8.0. Fourier Transform Infrared spectroscopy (FT-IR) spectra were recorded on a BRUKER EQUINOX 55 to determine the composition of the shell. The morphology and average particle size of the capsules were characterized using a Hitachi S-4300 scanning electronic microscope (SEM), operated at an accelerating voltage of 15 kV. Particle size and size distribution were also determined by a Malvern MasterSizer 2000 Particle Size Analyzer. DSC measurements were performed on a METTLER DSC822e differential scanning calorimeter in the range of 10–80 °C at a heating/cooling rate of 5 °C/min to evaluate the phase transition behavior. The diffraction patterns were obtained at the temperature of 25–60 °C by Synchrotron X-ray diffraction (XRD) on a PANalytical X'Pert Pro MPO instrument with TCU 2000 temperature control unit in Holland. The thermal stability of the capsules was studied in detail by observation under an Olympus optical microscopy equipped with a Linkam LTS350 hot stage at a scanning rate of 5 °C/min. The thermal decomposition of the capsules was characterized on a Perkin–Elmer Pysris 1 thermogravimetric analyzer (TGA) at a scanning rate of 10 °C/min under nitrogen.

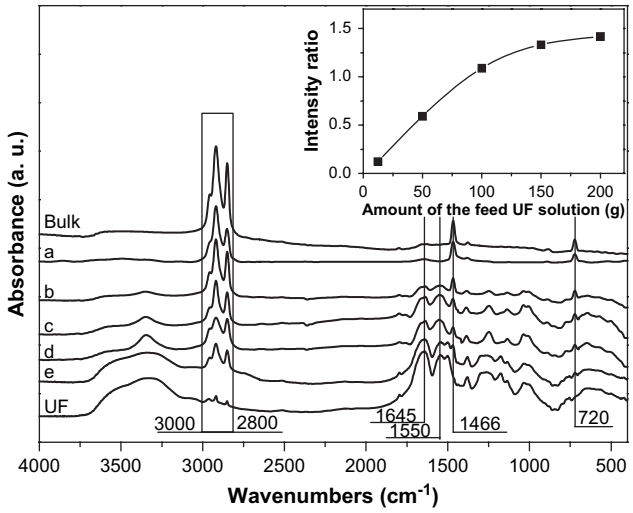

Fig. 2. FT-IR spectra of bulk paraffin, UF polymer and the capsules. The capsules were prepared at a fixed amount of HSMA solution 10.0 g as the emulsifier, 75 mL of water as a dispersion medium, 25.0 g of paraffin as the core material, but with varied feeding of the UF precursor solution forming the shell. (a) 12.5 g; (b) 50.0 g; (c) 100.0 g; (d) 150.0 g; (e) 200.0 g. Inset figure presents the intensity ratio of two characteristic peaks at 1645 cm^{-1} attributed to UF and at 1466 cm^{-1} attributed to paraffin, and the ratio dependence on the feeding amount of UF precursor solution.

3. Results and discussion

The synthesis scheme and structure of the emulsifier are illustrated in Fig. 1a. The yield of SMA is about 85%. The peaks at δ 3.0–3.8 ppm with the integral of 1.9512 and δ 6.5–7.8 ppm with the integral of 5.0000 (^{1}H NMR) are assigned to the protons in the succinic anhydride and benzene ring, respectively. The contents of styrene and maleic anhydride are calculated to be 50.6 wt% and 49.4 wt% according to the peak integral and their corresponding proton numbers. The near 1:1 ratio is consistent with the alternative copolymer characteristics. The peaks at δ 127–130 ppm with the integral of 5.088 and δ 135–140 ppm with the integral of 1.004 (^{13}C NMR) are assigned to carbons of benzene, and the peak at δ 170–174 ppm with the integral of 2.000 is assigned to carbon of succinic anhydride. The calculation of the peak integral and the carbon numbers gives a weight content of styrene and maleic anhydride 50.4 wt% and 49.6 wt%, respectively. Element analysis gives the contents of C and H element to be 71.82 wt% and 5.02 wt%, calculating that the weight contents of styrene and maleic anhydride are 51.2 wt% and 48.8 wt%, respectively. Since the homopolymerization of maleic anhydride is impossible, the results of ^{1}H NMR, ^{13}C NMR and element analysis all confirm that the resultant SMA should be alternative copolymer [29,30]. A GPC trace gives a molecular weight (M_n) of 1.06×10^4 and distribution of 2.6 of SMA. As shown in Fig. 1a, the hydrophobic group of phenyl and hydrophilic group of carboxyl arrange alternatively along the backbone, which will be conducive to a decrease of the interface tension between the oil and water. The polymeric emulsifier was further transformed into HSMA after being treated with NaOH to enhance its emulsification capability.

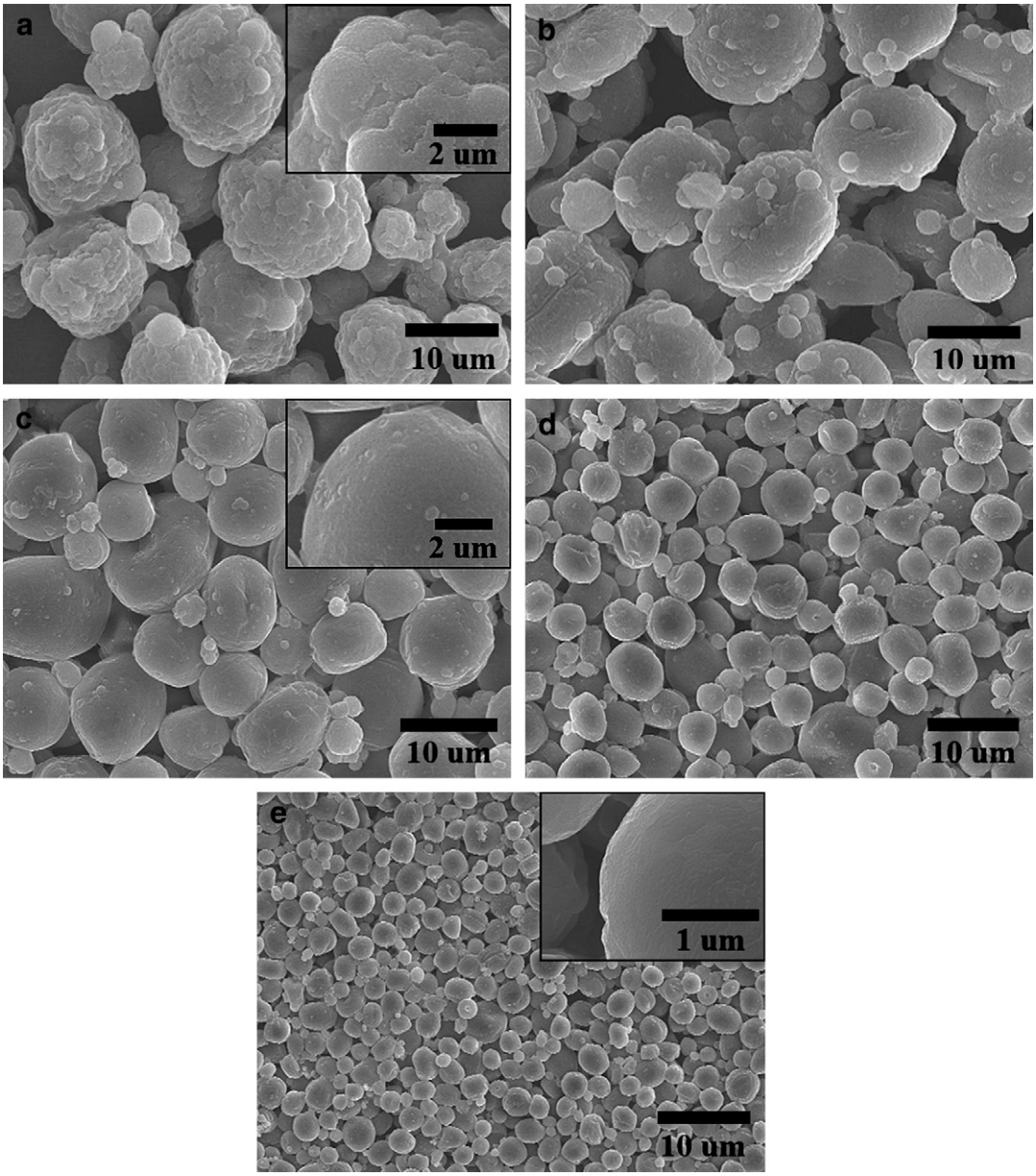

Fig. 3. Scanning electron microscopy images of the PCM capsules. They were prepared using a fixed amount of 50.0 g of UF precursor solution, 75 mL of water, 25.0 g of paraffin, but increased content of HSMA solution as emulsifier: (a) 2.5 g; (b) 5.0 g; (c) 10.0 g; (d) 15.0 g; (e) 20.0 g.

When HSMA molecules are adsorbed at the interfaces of paraffin oil droplets (see Fig. 1c), the charged region is exposed to aqueous media. This molecular arrangement results in better stability of the emulsion against coalescence. Such kind of molecular arrangement results in a relatively strong electronegative field at the surface of oil droplets, which can prevent oil droplets from coalescing. In fact, as shown in Fig. 1c, the zeta potential of the emulsion is −55.9 to −69.8 at pH value region 3.5–4.0. The melt paraffin emulsion in a hot water remained stable for several weeks. Besides enhances stability, the anionic HSMA would facilitate a favorable absorption of UF prepolymer by strong charged interaction and subsequent in situ polycondensation thereby creating the capsule walls with a compact shell.

The UF polymer is selected as the capsule shell due to its easier reaction and crosslink performance [31]. During the initial nucleophilic addition stage in Fig. 1b, formaldehyde (A) molecules react with urea (B) molecules in basic solution at pH 8.5 and 70 °C for about 1 h, giving UF prepolymer of some forms including monomethylol urea (C), dimethylol urea (D) and oligomer (E) (Fig. 1b). The linear or branched UF prepolymers are water soluble. These UF prepolymers are positively charged in acidic solution. After the UF was dropped into the paraffin emulsion at 70 °C, the anionic carboxyl group of HSMA induced a favorable absorption of UF prepolymer onto the interface by strong interaction (Fig. 1c). In acidic media, the positively charged UF prepolymer in the dispersion medium reacted to form larger molecules until the insoluble UF prepolymer deposited onto the surface of paraffin droplets. With the polycondensation procedure, UF polymer molecules were mainly crosslinked by methylene linkages forming compact shell. Owing to the property of UF polymer with the highly cross-linking structure, capsules with compact, integral and good mechanical strength are obtained.

The composition of the capsules was characterized as shown in Fig. 2. The multiple absorption peaks around 3000–2800 cm^{-1} are associated with the aliphatic C–H stretching vibration, the absorption peak at 1466 cm^{-1} is attributed to the C–H bending, and

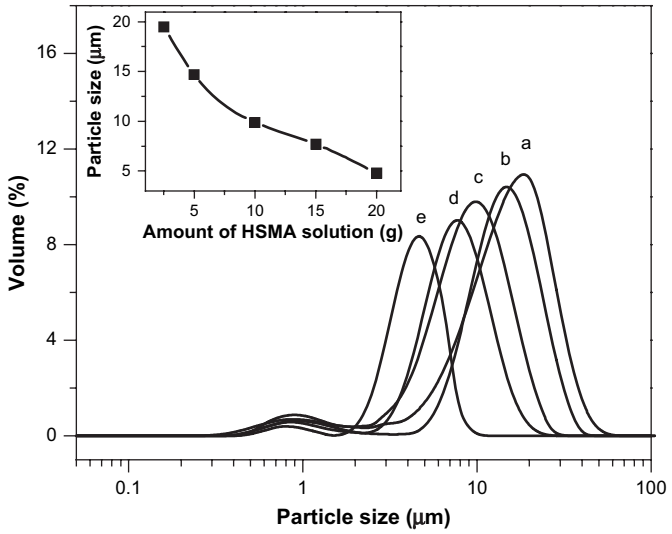

Fig. 4. Effect of HSMA solution content on particle size and distribution of the PCM capsules. They were prepared using a fixed amount of 50.0 g of UF precursor solution, 75 mL of water, 25.0 g of paraffin, but increased content of HSMA solution as emulsifier: (a) 2.5 g; (b) 5.0 g; (c) 10.0 g; (d) 15.0 g; (e) 20.0 g. Inset figure presents the average particle size dependences on the feeding amount of HSMA solution.

the absorption peak at 720 cm^{-1} is assigned to the group of CH_2 inplane vibration. These characteristic peaks represent the core material paraffin. The absorption peak at 1645 cm^{-1} is attributed to the –C═O stretching vibration, and the absorption peak at 1550 cm^{-1} is assigned to the group of –C–N– stretching vibration. These are characteristic peaks assigned to the shell material UF polymer. With the increased feeding of UF precursor, the peaks become stronger in intensity, meaning the increase of the shell (inset Fig. 2). The content of shell can be controlled by altering feeding amount of UF precursor. Besides the shell content, another important parameter particle size for the capsules was also systematically investigated.

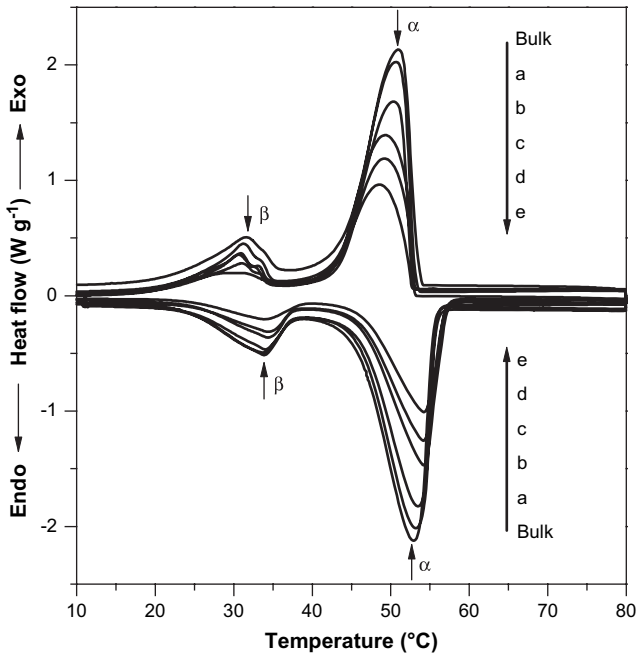

Fig. 5. DSC traces of bulk paraffin and the capsules at a given heating and cooling rate of 5 °C/min. The capsules were synthesized at a fixed amount of 10.0 g of HSMA, 75 mL of water, 25.0 g of paraffin, and increased feeding amount of UF precursor solution: (a) 12.5 g; (b) 50.0 g; (c) 100.0 g; (d) 150.0 g; (e) 200.0 g.

Table 1
Phase transition properties of the capsules from DSC measurements

Sample no.	Core content[a] (wt%)	ΔH_m (J g^{-1})	ΔH_c (J g^{-1})	T_m (°C)	T_c (°C)
Bulk	100	−204.8	203.7	53.2	50.5
1	97.9	−200.4	201.2	53.3	50.4
2	94.0	−192.6	195.3	53.4	50.2
3	83.3	−170.6	171.2	53.5	50.0
4	76.9	−157.5	158.4	53.9	49.8
5	72.0	−147.4	149.4	54.2	49.3
6	65.8	−134.7	139.6	54.2	49.2
7	59.9	−122.6	125.7	54.3	49.1
8	54.3	−111.2	114.3	54.3	49.0
9	48.1	−98.5	102.4	54.4	48.5

ΔH_m: the melting enthalpy; ΔH_c: the crystallization enthalpy; T_m: the melting temperature; T_c: the cooling temperature.

[a] The core content is calculated by the enthalpy of the capsules [21].

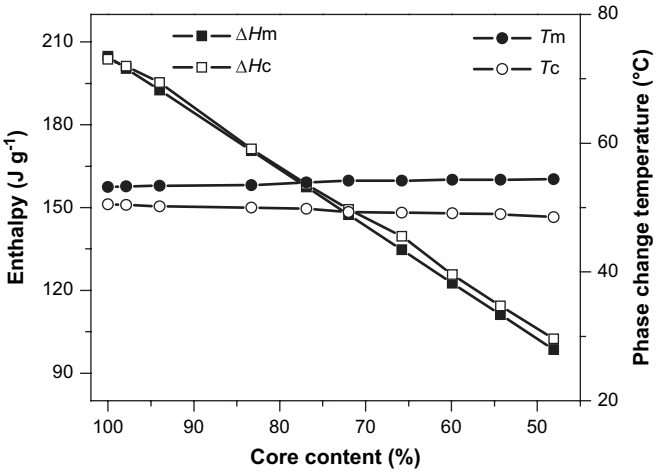

Fig. 6. Enthalpy and phase change temperature dependence of the capsules on the core content. The results are from Table 1. ΔH_m: the melting enthalpy; ΔH_c: the crystallization enthalpy; T_m: the melting temperature; T_c: the cooling temperature.

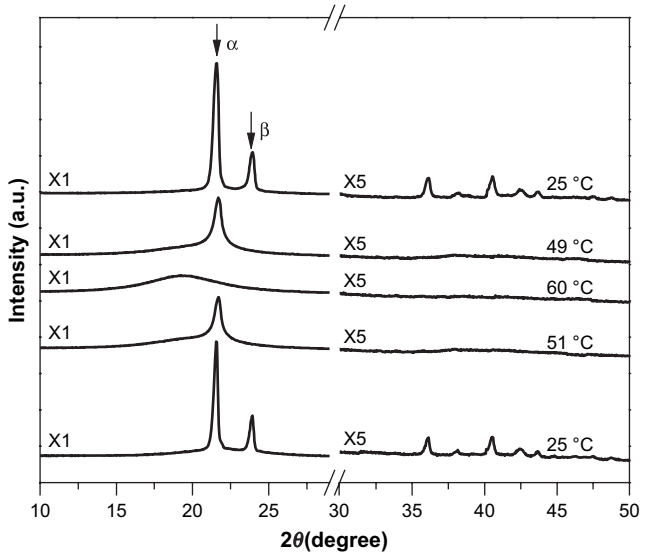

Fig. 7. X-ray diffraction patterns of the capsules containing 28.0 wt% shell content at different temperatures.

The particle size is very important in practical application, and herein it is mainly controlled by adjusting the feeding amount of HSMA at a given shell content. In Fig. 3, from (a–e), the particle size

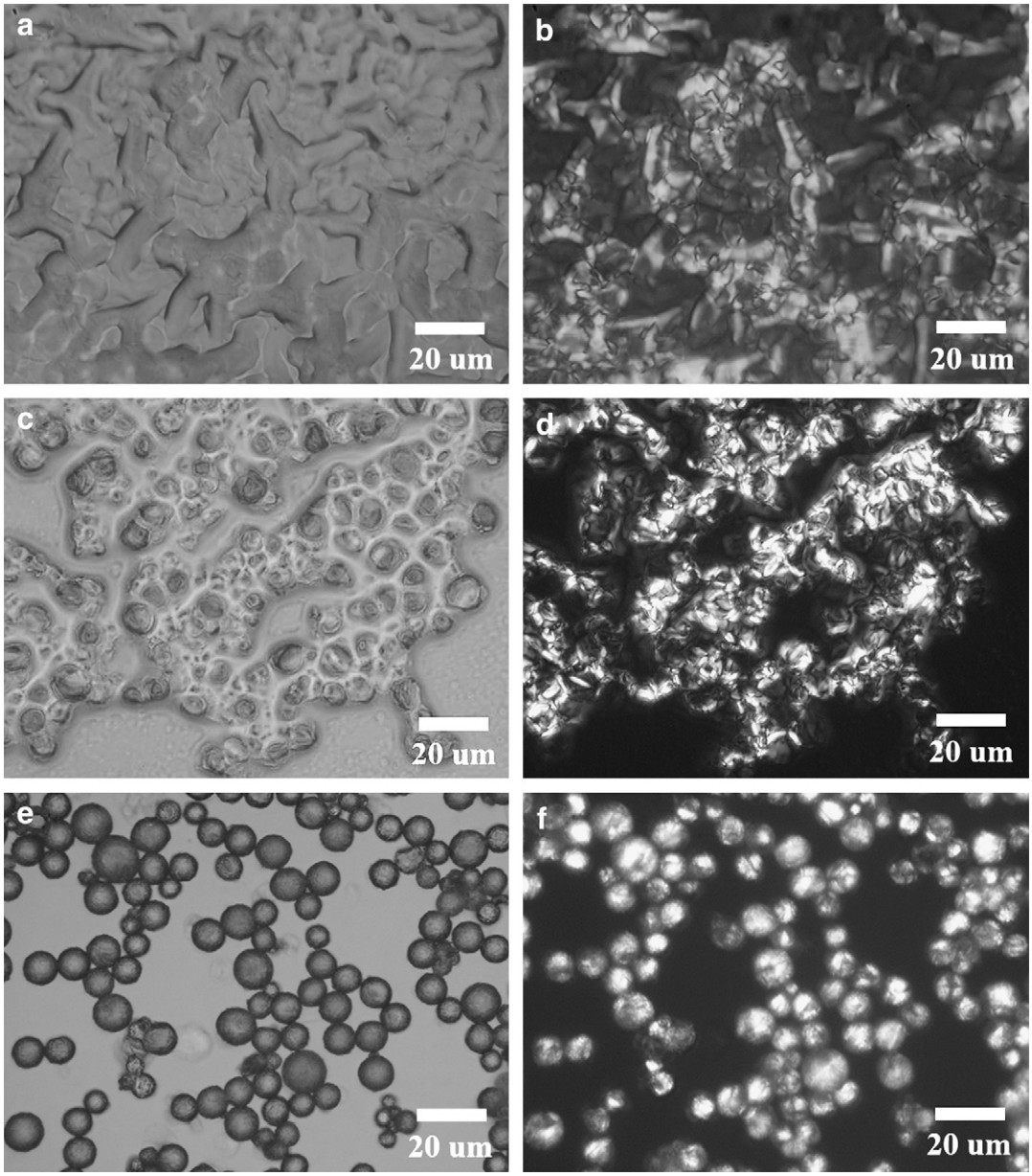

Fig. 8. Optical and polarized micrographs of the representative samples with varied shell content after being treated by heating to 60 °C thereafter cooling down to 25 °C. The capsules were synthesized at a fixed amount of 10.0 g of HSMA solution, 75 mL of water, 25.0 g of paraffin, and varied feeding amount of UF precursor solution: (a and b) 12.5 g; (c and d) 50.0 g; and (e and f) 100.0 g.

decreased with the increase of HSMA amount. The average particle diameter is 20 μm (Fig. 3a) when 2.5 g of HSMA solution was used, and the diameter decreased to about 5 μm (e) when 20 g of HSMA solution was used. Moreover, the capsules' surface becomes much smooth. Particle size and size distribution were also determined by a Malvern MasterSizer 2000 Particle Size Analyzer. Fig. 4 shows the effect of HSMA solution content on particle size and distribution of the PCM capsules. With increasing the amount of HSMA solution, the capsule average diameter decreased and their size distribution became narrower. The size analysis is consistent with SEM results.

It is important to retain as high enthalpy as possible of the capsules, whilst the capsules are not coalesced during melt/cooling cycles. Their thermal behavior was characterized by DSC analysis (Fig. 5). Two main transition peaks were clearly observed, in which α peak should be attributed to the heterogeneously nucleated rotator–liquid transition and β peak to the homogeneously nucleated crystal–rotator transition [22–24,32]. The enthalpy decreased with the increase of shell content, while the melt and freezing temperatures were slightly changed. The results are summarized in Table 1. As shown in Fig. 6, the enthalpy decreased linearly with the core content. On the other hand, the core content can be calculated from the enthalpy of the capsules [21], and then shell content is the relative residual.

Fig. 7 shows the X-ray diffraction patterns of the capsule containing 28.0 wt% shell content at different temperatures. At 25 °C, two main diffraction peaks of α and β were clear, indicating a high crystallization of the core paraffin. With the temperature increased gradually up to 51 °C, the β peak absolutely disappeared and the intensity of α peak decreased remarkably, clearly indicating the completion of whole crystal–rotator transition and part of rotator–liquid transition. At 60 °C, no characteristic diffraction peaks were found except for a broad scattering peak owing to amorphous UF polymer, indicating a complete melt of the core paraffin. When the temperature decreased gradually up to 49 °C, the α peak appeared,

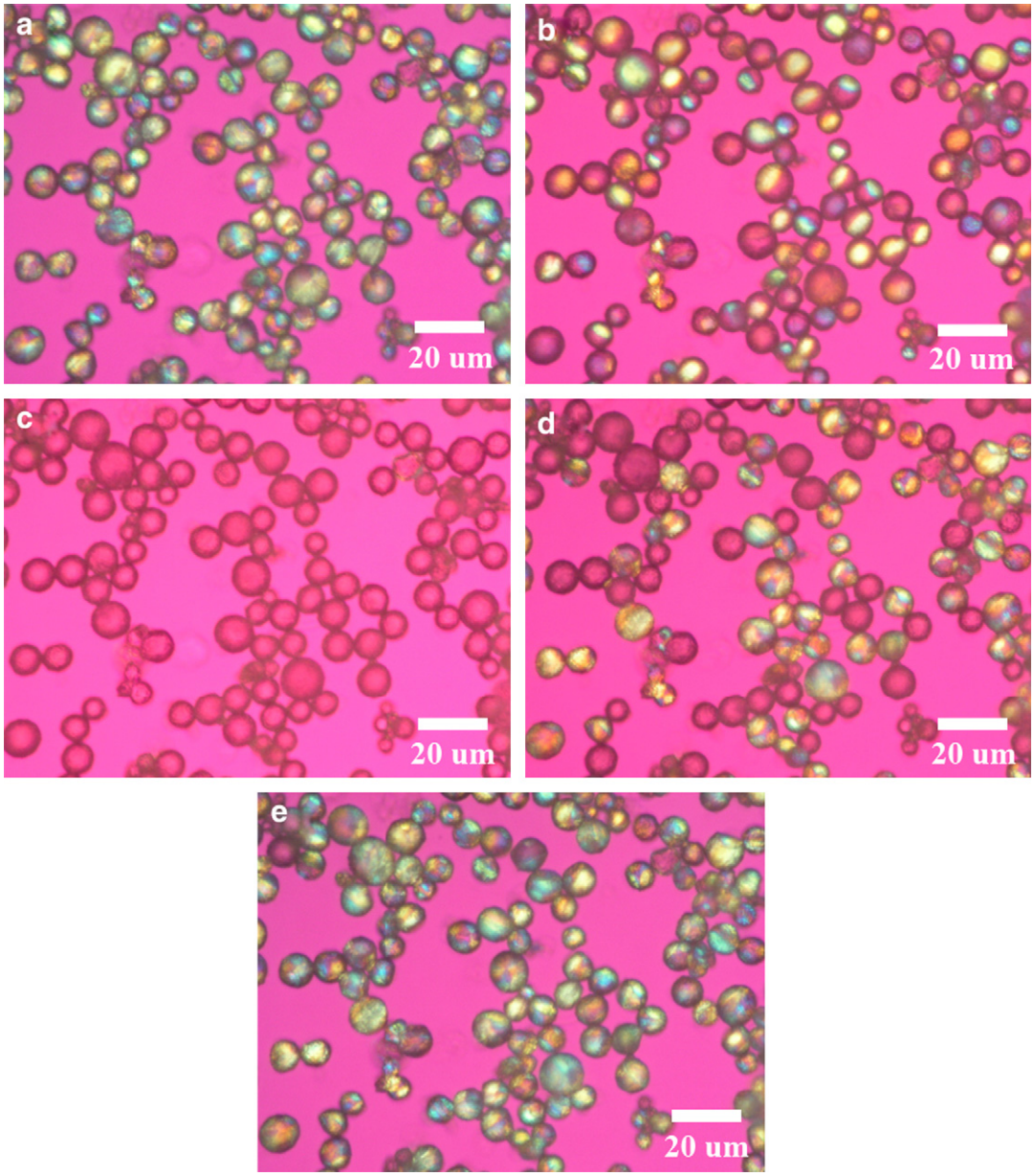

Fig. 9. Polarized optical micrographs of the capsule containing 28.0 wt% shell content at some representative temperature stages: (a) 25 °C; (b) 54 °C; (c) 60 °C; (d) 50 °C; (e) 25 °C.

indicating a partial crystallization of the core paraffin. At a lower temperature of 25 °C, the α and β peaks clearly appeared, suggesting the completion of liquid–rotator transition and rotator–crystal transition. The XRD results are consistent with the above DSC results.

In order to evaluate the thermal stability of the PCM capsules during the phase transition, the morphological evolution was observed under a polarized optical microscope at a temperature scanning rate of 5 °C/min within 25–60 °C. As seen in Fig. 8a and b, the capsules were completely coalesced when the shell content was rather low for example 2.1 wt%. This can be understood by the leakage of the melt paraffin core from the cracked shell. When the shell content was increased to 16.7 wt% (Fig. 8c and d), the capsules were partially coalesced with the spherical contour distinguished. When the shell content was increased up to 28.0 wt% (Fig. 8e and f), the capsules were intact while the solid powder form was well retained after many melting/crystallization cycles. In order to further characterize the phase transition of the capsules, the morphology of a representative capsule was observed at different temperatures (Fig. 9). At a low temperature 25 °C, the capsules were in individual spherical shape with a clear core–shell structure (Fig. 9a). The colorful texture was clearly discerned, indicating the interior paraffin core was crystalline. With the temperature increased gradually up to 54 °C, the capsules started to partially melt (Fig. 9b). At 60 °C, no colorful texture was observed, indicating a complete melt of the core paraffin (Fig. 9c). It should be noticed that the capsules remained individually without any coalescence. With the temperature decreased up to 50 °C, the melt core paraffin started to partially crystallize (Fig. 9d). At a lower temperature for example 25 °C, the crystallization degree increased remarkably (Fig. 9e) with the capsules intact remained. The polarized optical microscopy results are consistent with the above DSC and XRD results.

The thermal decomposition of the capsules was characterized by TGA (Fig. 10). All the capsules have no mass loss at high

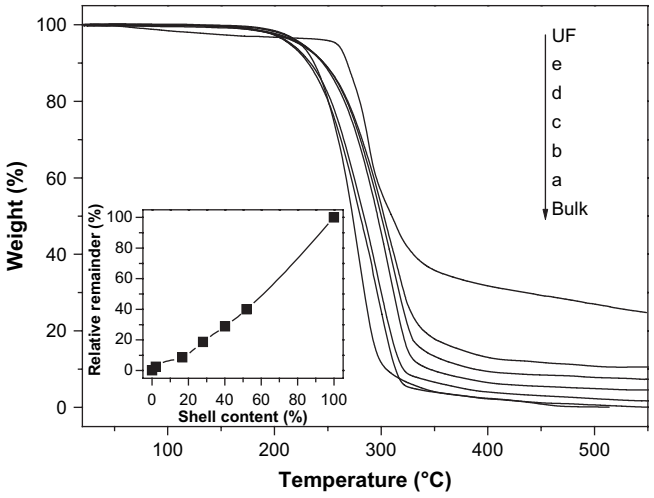

Fig. 10. TGA diagrams of the capsules with varied shell content, the same as shown in Fig. 3. Inset figure correlates the shell content and reduced residual mass at 500 °C to that of pure UF polymer.

temperature 200 °C. There existed a remarkable mass loss for the bulk paraffin at 250 °C. Up to 500 °C, the paraffin was completely lost. For the capsules, the onset temperature was slightly increased, while there existed mass residual at 500 °C. With the increase of the shell content, the residual mass was increased as shown in inset Fig. 10. The good thermal stability is important in practical applications especially for melt processing.

4. Conclusions

In conclusion, the capsules containing high melt temperature paraffin as a representative phase change material have been synthesized by in situ encapsulation by polymerization of urea–formaldehyde precursor. The particles' size, size distribution and shell content can be controlled. The capsules are sufficiently robust to keep the powder form unchanged after heating/cooling cycles, meanwhile the thermal capacity keeps a high level due to the high crystallization of the core paraffin. The method can be extended to such paraffin samples with a broad melt temperature tunable ranging from higher temperature to ambient temperature. The PCM capsules will be potentially useful in energy conservation, functional heat fluid and heat protection materials.

Acknowledgments

The authors are thankful to the NSF of China (50573083, 50733004, 50521302, 90606031 and 20720102041).

References

[1] Zalba B, Marín JM, Cabeza LF, Mehling H. Applied Thermal Engineering 2003; 23:251.
[2] Himran S, Suwono A, Mansoori GA. Energy Sources 1994;16:117.
[3] Ying BA, Kwok YL, Li Y, Zhu QY, Yeung CY. Polymer Testing 2004;23: 541.
[4] Kim J, Cho G. Textile Research Journal 2002;72:1093.
[5] Sarier N, Onder E. Thermochimica Acta 2007;452:149.
[6] Shin Y, Yoo DI, Son K. Journal of Applied Polymer Science 2005;96: 2005.
[7] Shin Y, Yoo DI, Son K. Journal of Applied Polymer Science 2005;97:910.
[8] Shilei L, Feng GH, Neng Z, Li DY. Energy and Building 2007;39:1088.
[9] Schossig P, Henning HM, Gschwander S, Haussmann T. Solar Energy Materials and Solar Cells 2005;89:297.
[10] Brown RC, Rasberry JD, Overmann SP. Powder Technology 1998;98:217.
[11] Yamagishi Y, Takeuchi H, Pyatenko AT, Kayukawa N. AIChE Journal 1999;45: 696.
[12] Hawlader MNA, Uddin MS, Zhu HJ. International Journal of Energy Research 2002;26:159.
[13] Rossi RM, Bolli WP. Advanced Engineering Materials 2005;7:368.
[14] Chen CZ, Wang LG, Huang Y. Polymer 2007;48:5202.
[15] Yuan L, Liang GZ, Xie JQ. Colloid and Polymer Science 2007;285:781.
[16] Yin T, Rong MZ, Zhang MQ, Yang GC. Composites Science and Technology 2007;67:201.
[17] Yuan L, Liang GZ, Xie JQ, Li L, Guo J. Polymer 2006;47:5338.
[18] Su JF, Wang LX, Ren L. Colloids and Surfaces A 2007;299:268.
[19] Cho JS, Kwon A, Cho CG. Colloid and Polymer Science 2002;280:260.
[20] Hawlader MNA, Uddin MS, Zhu HJ. International Journal of Solar Energy 2000; 20:227.
[21] Zhang XX, Fan YF, Tao XM, Yick KL. Materials Chemistry and Physics 2004;88: 300.
[22] Zhang XX, Tao XM, Yick KL, Fan YF. Journal of Applied Polymer Science 2005; 97:390.
[23] Fan YF, Zhang XX, Wang XC, Li J, Zhu QB. Thermochimica Acta 2004;413:1.
[24] Fan YF, Zhang XX, Wu SZ, Wang XC. Thermochimica Acta 2005;429:25.
[25] Zhang XX, Fan YF, Tao XM, Yick KL. Journal of Colloid and Interface Science 2005;281:299.
[26] Zhang XX, Tao XM, Yick KL, Wang XC. Colloid and Polymer Science 2004;282: 330.
[27] Song QW, Li Y, Xing JW, Hu JY, Marcus Y. Polymer 2007;48:3317.
[28] Mulligan JC, Colvin DP, Bryant YG. Journal of Spacecraft and Rocket Report 1996;33:278.
[29] Soer WJ, Ming WH, Klumperman B, Koning C, Benthem RV. Polymer 2006;47: 7621.
[30] Shulkin A, Stöver HDH. Journal of Membrane Science 2002;209:421.
[31] Rammon RM, Johns WE, Magnuson J, Dunker AK. The Journal of Adhesion 1986;19:115.
[32] Xie BQ, Shi H, Jiang SC, Zhao Y, Han CC, Xu DF, et al. Journal of Physical Chemistry B 2006;110:14279.